2005

Evaluation of Toxic Agent Effects on Lung Cells by Fiber Evanescent Wave Spectroscopy

Pierre Lucas
University of Arizona, pierre@email.arizona.edu

David Lee Coq
Universite du Littoral

Christophe Juncker
University of Arizona

Jayne Collier
University of Arizona

Dianne E. Boesewetter
University of Arizona

See next page for additional authors

Evaluation of Toxic Agent Effects on Lung Cells by Fiber Evanescent Wave Spectroscopy

PIERRE LUCAS,* DAVID LE COQ, CHRISTOPHE JUNCKER, JAYNE COLLIER, DIANNE E. BOESEWETTER, CATHERINE BOUSSARD-PLÉDEL, BRUNO BUREAU, and MARK R. RILEY

Department of Material Science and Engineering, University of Arizona, Tucson, Arizona 85721 (P.L., C.J.); Laboratoire de physicochimie de l'atmosphère, Universite du Littoral, 59140 Dunkerque, France (D.L.C.); Department of Agricultural and Biosystems Engineering, University of Arizona, Tucson, Arizona 85721 (J.C., D.E.B., M.R.R.); and Laboratoire des Verres et Céramiques, UMR-CNRS 6512, Université de Rennes 1 Campus de Beaulieu, 35042 Rennes, France (C.B.-P., B.B.)

Biochemical changes in living cells are detected using a fiber probe system composed of a single chalcogenide fiber acting as both the sensor and transmission line for infrared optical signals. The signal is collected via evanescent wave absorption along the tapered sensing zone of the fiber. We spectroscopically monitored the effects of the surfactant Triton X-100, which serves as a toxic agent simulant on a transformed human lung carcinoma type II epithelial cell line (A549). We observe spectral changes between 2800–3000 cm^{-1} in four absorptions bands, which are assigned to hydrocarbon vibrations of methylene and methyl groups in membrane lipids. Comparison of fiber and transmission spectra shows that the present technique allows one to locally probe the cell plasma membrane in the lipid spectral region. These optical responses are correlated with cellular metabolic activity measurements and LDH (lactate dehydrogenase) release assays that indicate a loss of cellular function and membrane integrity as would be expected in response to the membrane solubilizing Triton. The spectroscopic technique shows a significantly greater detection resolution in time and concentration.

Index Headings: **Fourier transform infrared spectroscopy; FT-IR spectroscopy; Chalcogenide glass fiber; Human lung cells; Cell culture; Toxicity monitoring.**

INTRODUCTION

Fourier transform infrared (FT-IR) spectroscopy is recognized as a powerful, nondestructive technique for probing and identifying biomolecules and characterizing individual cells.[1,2] The spectral range of FT-IR allows one to probe the fundamental vibrational modes of functional groups existing in biomolecules and can provide a highly specific vibrational fingerprint of microorganisms. Spectral features from the fingerprint region between 400–4000 cm^{-1} can supply information about the components as well as the conformation of cellular components. FT-IR spectroscopy not only permits observation of changes occurring at the molecular level within the cell but it is also very rapid and requires no reagents. Infrared spectroscopy has been applied to evaluate the biochemical composition of mammalian cells or to discriminate between cancerous and healthy cells.[2–4] While discriminations can be made between stages of the cell cycle due to alterations in spectral signatures of nucleic acids,[5] only very small differences are apparent between distinct subcellular structures. Analyses of separate cell fractions, isolated by sucrose density gradient centrifugation, present the most significant spectral differences in the C–H stretching region (2800–3000 cm^{-1}), at the ester carbonyl stretching band (1737 cm^{-1}), and in the PO_2^- stretching region (1089 and 1242 cm^{-1}).[2]

In this study, we use a fiber based optical biosensor operating in the mid-infrared. This optical sensor makes use of an infrared (IR) glass fiber as both a waveguide and sensing element, which permits remote collection of IR spectra. The fibers used for collecting IR data are made from chalcogenide glasses based on tellurium, arsenic, and selenium. The selected $Te_2As_3Se_5$ (TAS) composition is very suitable since it has an excellent resistance to devitrification and shows a good chemical durability, notably toward water. The transparency domain of these fibers, 800 to 4000 cm^{-1}, is very attractive as it corresponds to the region of strong fundamental vibrational modes of organic and biologically relevant molecules including lipids, proteins, and nucleic acids. The principle of measurement is based on the general concept of fiber evanescent wave spectroscopy (FEWS).[6,7] When the lightwave is guided through the fiber, part of its E field extends outside the surface and constitutes the evanescent wave. The detection principle of these optical fiber sensors is based on the absorption of the evanescent wave by substances in contact with the fiber surface. This technique yields IR data very similar to that obtained with attenuated total reflectance (ATR) spectroscopy.

Fiber based sensors can be used for monitoring biological processes *in situ* and therefore have potential for developing innovative endoscopic tools. Keirsse et al. used FEWS to identify metabolic changes in starved mice liver tissue and also monitored the dynamics of bacterial biofilms in real time.[8] The technique allows observation of metabolic changes at the molecular level, including a rise of triglyceride content in liver cells and release of polysaccharides during bacterial swarming.

In this work, we report spectral changes for alveolar epithelial cells after exposure to a toxic agent. These cells play an important role in the response of the lung to injury as they serve as the primary barrier between breathable air and the blood stream and due to their function of synthesizing and secreting pulmonary surfactant, by acting as the stem cell for replacement of type I epithelial cells,[9] and through secretion of chemokines.[10] In this work, the cell response is studied by monitoring the spectral absorptions located between 2800–3000 cm^{-1}

Received 28 July 2004; accepted 25 August 2004.

* Author to whom correspondence should be sent. E-mail: pierre@u.arizona.edu.

0003-7028/05/5901-0001$2.00/0

due to hydrocarbon vibrations of methyl and methylene groups in membrane lipids. The cells are maintained at near to complete confluence (full coverage of their attachment surface), which inhibits cell replication and thus reduces variations from cell to cell in their stage of the growth cycle. When a cytotoxic compound interacts with an epithelial cell, the cell may alter its metabolism (often involving a redistribution of energy to produce a variety of response proteins), may secrete cytokines, or may suffer irreparable damage to vital components including the cell membrane, protein channels, DNA, or the cytoarchitechture. The metabolism of this epithelial layer is often one of the first cellular functions altered by the presence of toxins.[11] The surfactant Triton X-100 was used as a model toxic agent as this disrupts cell membranes and causes rapid cell death when present at sufficiently high concentrations, but at levels below those used for total solubilization of cellular matter.

EXPERIMENTAL METHODS

Cell Culture. A transformed, immortalized alveolar carcinoma type II epithelial cell line (A549) obtained from American Type Culture Collection (ATCC) from human origin was maintained in DME media (Sigma Chemical Co., St. Louis, MO), supplemented with 10% fetal bovine serum and 1% antibiotic-antimycotic solution (Sigma, St. Louis, MO), at 37 °C and 5% CO_2. Cellular response assays of cell metabolism and cell death were performed after 2 to 24 h of continual exposure to Triton.

For cytotoxicity experiments, newly confluent cell layers were trypsinized, from a 25 cm^2 T-flask, resuspended in medium, and seeded in 96-well plates with 100 μL/well. Plates were seed with 12 500 cells per well, which corresponds to 25% confluence over each well in the plate, and then allowed to grow to confluence for 48 h at 37 °C and 5% CO_2. After 48 h of growth, the number of cells per well was approximately 50 000 at 100% confluence.

One of the goals of this work was to collect the IR signatures of viable and metabolically active lung cells and to follow the change in their optical signatures when the surfactant Triton was introduced in the solution. All exposures to Triton and control culture measurements were performed in serum free medium as some biological toxins have previously been found to bind strongly to serum proteins.[12] The serum was washed from the cell layers by gently removing the seeding medium with a pipette and then adding 120 μL/well of serum free DMEM-F12. This rinsing medium was incubated for 30 min and then the process was repeated once again. Exposures were typically performed with 16 replicates (two columns of a 96-well plate). The final rinsing medium was removed, and 100 μL of the toxic solution was added. The stock solution of the Triton was dissolved in 10 mM PBS (phosphate buffered saline), pH 7.4, to yield a concentration 10 times greater than the concentration of interest. The final Triton solution consisted of 10% of the stock and 90% serum free medium with 1% antibiotic-antimycotic solution (Sigma Chemical Co., St. Louis, MO). All Triton solutions were prepared fresh on the day of the exposure. Two columns of the 96-well plate (16 wells) were devoted to an unexposed control.

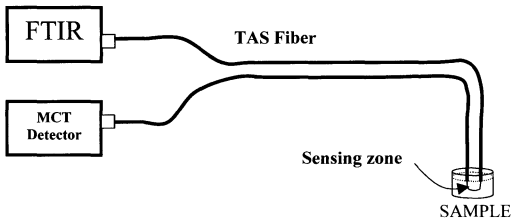

FIG. 1. Schematic representation of the experimental setup used for FEWS experiments.

Spectroscopic Measurements. To manufacture infrared fibers, preforms of $Te_2As_3Se_5$ (TAS) glasses were prepared using a previously described fabrication process.[7] The main steps consist of purifying the starting elements, distilling the element mixture at high temperature, homogenizing the glass in a silica tube using a rocking furnace, and quenching the silica tube to obtain a rod. In order to eliminate the internal constraints due to quenching, the preform was annealed at a temperature close to the glass temperature (T_g = 137 °C). The resulting preform was then drawn into a fiber with a diameter of approximately 400 μm, as described in Ref. 7. During this drawing process, the fiber diameter was locally reduced from 400 μm to 100 μm along sections 20 cm in length by controlling the drawing speed and the heating zone of the glass preform. This part of the fiber constitutes the sensing zone. It is well known that a local reduction of the fiber diameter increases the optical sensitivity of the fiber.[13,14] The fibers used for the experiments have an overall length of 50 cm, including the length of the sensing zone.

Experiments were carried out with a Tensor 27 Bruker FTIR coupled to the tapered fiber and an external mercury cadmium telluride (MCT) IR detector. The sensing zone of the fiber is designed as a U-turn, which is dipped in a 250 μL Pyrex chamber containing the sample to be analyzed. Figure 1 displays a schematic of this experimental setup. The measurements were carried out at room temperature. Spectra were obtained at 4 cm^{-1} resolution with 400 scans taken per spectrum. Every resulting spectrum was baseline corrected using Bruker's proprietary software, OPUS. The first step of the experiments consisted of recording a reference spectrum after dipping the tapered sensing zone of the fiber into the 250 μL Pyrex chamber containing a 0.9% NaCl solution. The cell spectra were subsequently recorded with the same fiber after introducing the pellet of human lung cells (A549) in the chamber. The absorption of the cells was calculated as shown in Eq. 1, where I_{NaCl} is the intensity of the 0.9% NaCl spectrum and I_{cells} is the intensity measured when the cells are in the chamber.

$$Absorbance = -\log\left(\frac{I_{cells}}{I_{NaCl}}\right) \quad (1)$$

The length of contact between the fiber and the analyzed solutions critically affects the FEWS data;[15] therefore, the same contact length was strictly used for reference and sample spectra. The cells were allowed to attach

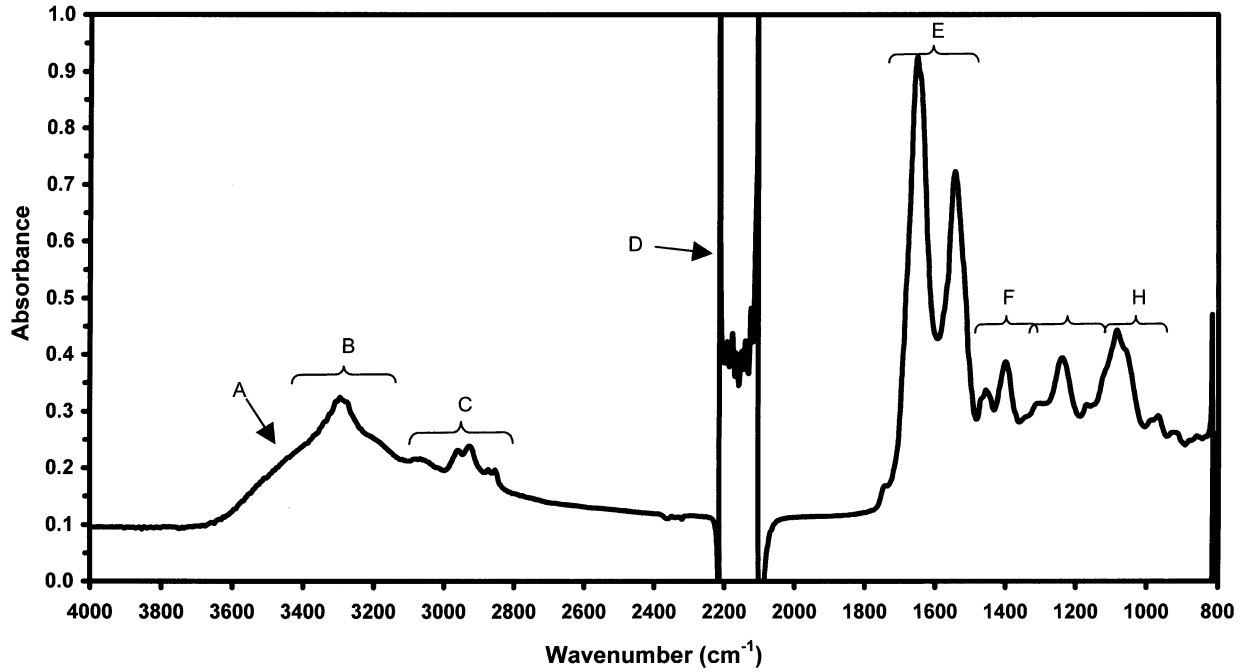

FIG. 2. Typical FEWS spectrum of human lung cells from a TAS fiber. The figure exhibits several spectral regions as follow: (*A*) O–H elongation of water, (*B*) amide A and B of proteins, (*C*) CH_2, CH_3 of lipids, (*D*) saturation due to Se–H bonds from the TAS fiber, (*E*) amide I and II of proteins, (*F*) fatty acids and amino acids, (*G*) phospholipids and nucleic acids, and (*H*) polysaccharides.

to the fiber for two hours before the toxic agent was added into the Pyrex chamber.

Figure 2 shows the IR spectrum collected by FEWS of healthy cells coated on the fiber in air for 2 min. The spectrum underlines the validity of the technique for studying biological compounds. The common spectral features expected for biological samples are assigned as follow: O–H elongation of water (A), amide A and B of proteins (B), CH_2 and CH_3 of lipids (C), amide I and II of proteins (E), fatty acids and amino acids (F), phospholipids and nucleic acids (G), and polysaccharides (H). In this figure, the saturation located at 2200 cm^{-1} (D) is due to Se–H bonds from the TAS fiber.

For comparison purposes, transmission FT-IR measurements were performed on the A549 cells under the same conditions as the FEWS experiment. The chamber for transmission had a fixed optical path composed of two CaF windows held at a constant distance with a 25 μm thick Teflon separator. Healthy cells and cells with 1 mM Triton in 0.9% NaCl were introduced in the chamber and monitored over time. The 0.9% NaCl solution was used as a background.

The A549 type II alveolar epithelial cells used in this study are an anchorage-dependent immortalized lung cell line that form strong attachments to surfaces. It is critical for the FEWS experiment that the cells generate a strong contact with the sensing zone of the TAS fiber. The ability of lung cells to adhere to the fiber surface and to live in contact with the fiber was investigated by optical microscopy and fluorescence imaging. To measure the viability of A549s growing on fibers, a fluorescence assay was performed using the LIVE/DEAD Reduced Biohazard Viability/Cytotoxicity Kit #1 from Molecular Probes, Inc. (Eugene, OR). Cells on fibers were incubated for fifteen minutes in darkness at room temperature with two fluorescent dyes, each as a 1:500 dilution of stock material with HEPES-buffered saline solution. SYTO 10 green fluorescent nucleic acid stain stains viable cells. The Dead Red nucleic acid dye stains non-viable cells.

Cytotoxicity Quantification. For evaluation of cytotoxicity, cells were exposed for various times ranging from 2 to 24 h before quantification of cell viability. Cellular metabolism was evaluated using an MTT (3(4,5-dimethylthiazol-2-yl) 2,5-diphenyltetrazolium bromide) assay on the epithelial cells. This tetrazolium salt is cleaved to formazan by the succinate-tetrazolium reductase system in active mitochondria.[16] The colorimetric assay correlates the amount of formazan dye produced to the metabolic activity of the cells. More information may be found in Riley et al.[17]

Cell death was quantified using a commercial non-radioactive LDH (lactate dehydrogenase) release assay (Roche Diagnostics GmbH, Mannheim, Germany) and followed manufacturer's procedures. LDH release is an indicator of damage to plasma membrane integrity. The LDH activity was determined by adding 100 μL of the kit reaction mixture to each well of the 96-well plate on top of the cell solution already exposed for the desired time. This was incubated for 30 min at room temperature protected from light and then read at 492 nm on a plate reader. Experimental cultures exposed to Triton were compared to controls of non-exposed cultures and cultures lysed using the surfactant tween-20 to solubilize cell membranes and release intracellular LDH. Lysed cell LDH levels were assumed to represent 100% cell death. As each exposure was performed with confluent monolayers of cells, total available LDH was consistent across experiments. Each measurement was performed with at least 8 replicates.

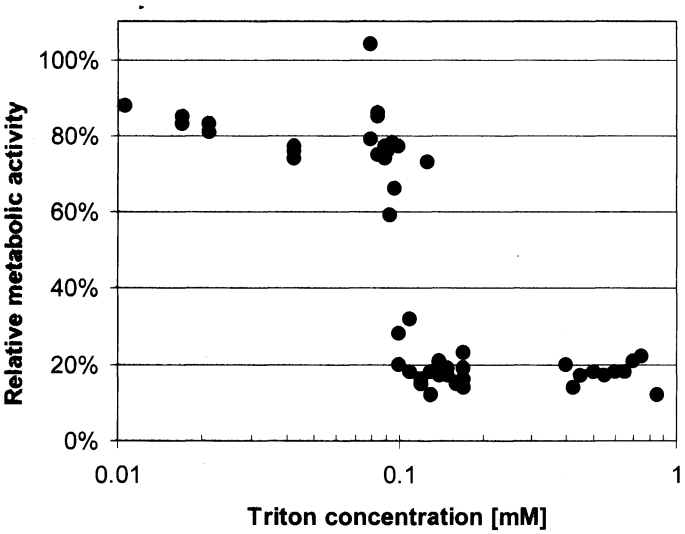

FIG. 3. Relative metabolic activity of A549 cells exposed to Triton for 24 h compared to unexposed control A549 cells. Error bars not shown for clarity; standard deviations are typically 5–7% of measurement value.

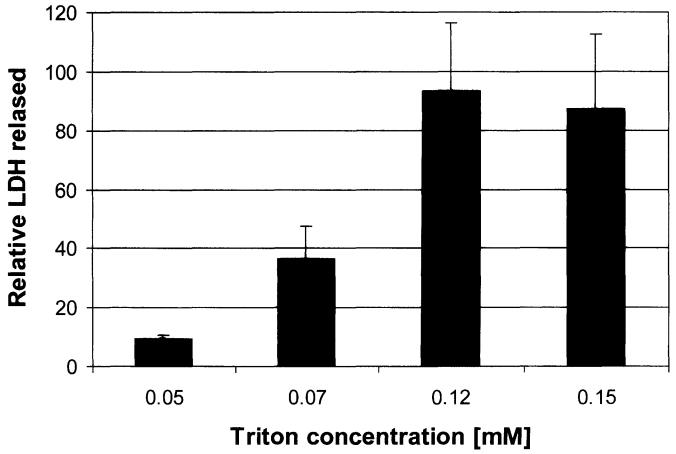

FIG. 4. Release of LDH (lactate dehydrogenase) after 2.5 h, compared to unexposed control. LDH release is commonly used as an indicator of the integrity of a cell membrane.

RESULTS

The sensitivity of the A549 lung cells to varying amounts of Triton was evaluated for 24 h exposures. The relative metabolic activity is presented in Fig. 3 for Triton concentrations from 0.01 to 1.0 mM. Healthy cultures would have a relative metabolic activity of 100; dead or damaged cell cultures would have an activity below 20, the lower bound of the assay.

The dose response relation of A549s to varying Triton concentrations follows nearly a step change decrease. This is somewhat unusual as the A549 cells usually respond with a slow decline in culture health with increasing concentration of a stressor.[17] The behavior observed here is related to the critical micelle concentration of Triton, which is approximately 0.26 mM.[18] Below this, Triton causes only minimal damage; above this concentration Triton solubilizes portions of the cell membrane, leaving holes through which intracellular compounds may pass. This mechanism is supported by measurements of the release of LDH, normally an intracellular enzyme (Fig. 4). Only a small amount of LDH is present in the culture media upon exposure of the cells to 0.05 mM. Exposure to 0.07 mM leads to some release, indicative of damage to a moderate number of cells. Exposure to higher amounts of Triton leads to the release of nearly all the available LDH, indicative of loss of membrane integrity by most cells.

These biochemical analyses provide information on the concentration sensitivity of the A549 cells and on mechanisms and timing of damage resulting from exposure to a surfactant such as Triton. The presence of some residual metabolic activity even when significant amounts of LDH are released indicates that membrane damage occurs at an earlier time than do intracellular changes to cellular functions such as metabolism. The information from these biochemical analyses was used to select the Triton concentrations and time of evaluation for the spectroscopic analyses.

Figure 5 shows fluorescence images and a bright field micrograph of the fiber covered with lung cells. These images illustrate that cells do attach to the fiber surface and are mostly deposited in a uniform layer. Nearly confluent coverage is obtained with cell attachment to the fibers. A majority of the cells maintain viability at the fiber surface. The conditions of cell attachment and homogeneous distribution are ideal for the FEWS experiment. These cells are approximately 10 μm in diameter and approximately 3–4 μm in height and they form tight connections to surfaces through focal contacts. The membrane-to-surface separation distance varies from 10 to 20 nm at the adhesion site, to up to 200 nm for other areas of the cell.

Upon exposure to Triton, the A549 cells undergo a slow physiological change as displayed in Fig. 6. When exposed to low concentrations of Triton (0.025 mM) for up to 60 min (b), cell morphology changes little compared to that of unexposed controls (a). Both images display normal cuboidal cell morphology with tight connections to the surface. After exposure to 0.1 mM Triton for 60 min (Fig. 6c), the cells begin to lose their tight packing and appear to be more round; however, nearly all cells remain attached for at least 120 min (not shown). Exposure to very high Triton concentrations of 0.25 mM (Fig. 6d) shows a substantial change in morphology with an increase in the rounding of cells. Nearly all cells remain attached to the surface with a loss of cell coverage only on the order of 5%.

Figure 7 demonstrates that cells stay attached to the chalcogenide fiber during the full course of the FEWS experiment. The figure shows the tapered portion of the fiber after completion of the experiment and confirms that even after four hours of exposure to 1 mM Triton the cells still maintain a monolayer at the fiber surface.

The FEWS spectra of viable A549 human lung cells are shown in Fig. 8a for the range 2800–3050 cm^{-1}, corresponding to membrane lipids. Several cell spectra collected over increasing periods of time are plotted on the same figure and are shown to superimpose. This plot indicates that the spectral signatures of live cells do not change during the first hour and only exhibit a slight decrease in intensity after four hours. These spectroscopic data corroborate the fluorescence data in showing that the

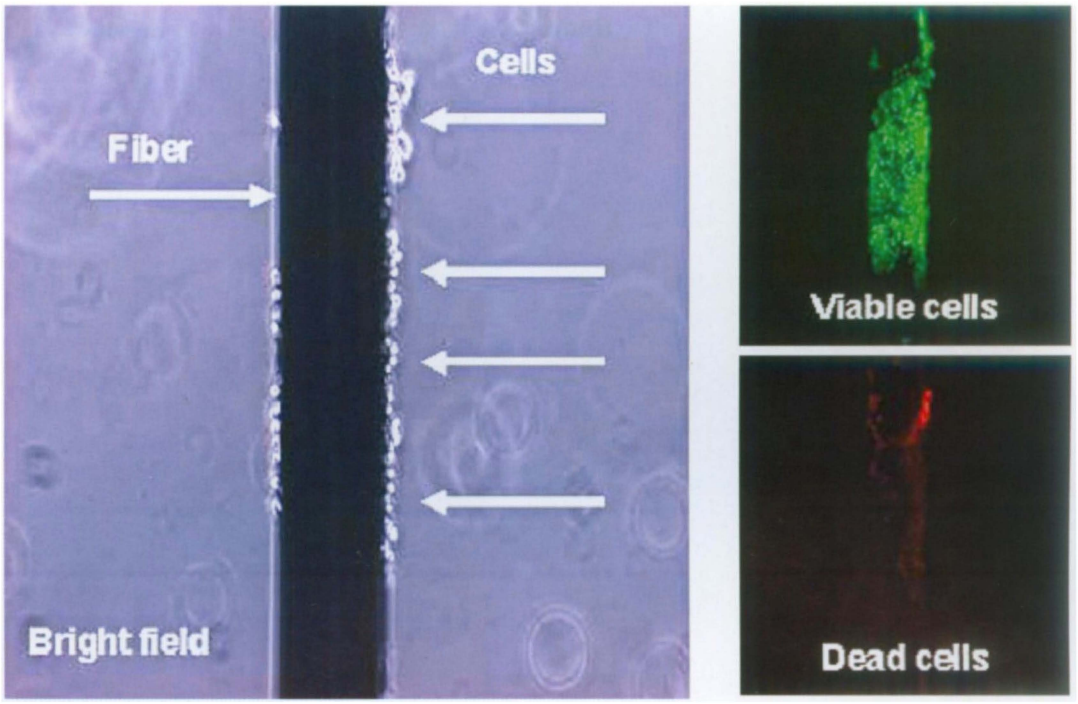

FIG. 5. Optical photomicrographs of a chalcogenide fiber after cell attachment. Each image shows the same field. Image on the left hand side employed bright field microscopy, and images on the right show fluorescence photomicrographs with cells labeled with two dyes; green on the top indicates viable cells, red on the bottom image indicates non-viable cells.

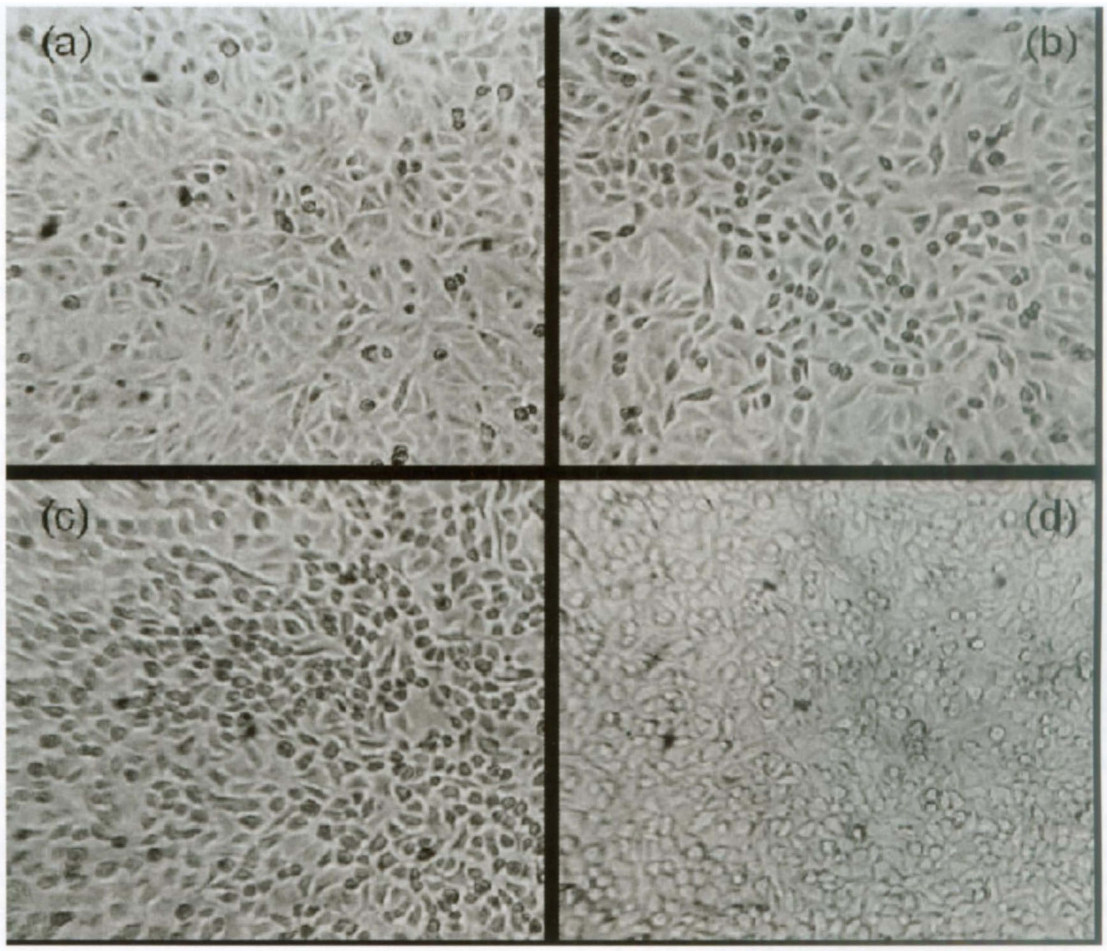

FIG. 6. Photomicrographs of A549 cells on plastic tissue culture dishes after 60 min of exposure to Triton. (**a**) Control, (**b**) 0.025 mM Triton, (**c**) 0.1 mM Triton, and (**d**) 0.25 mM Triton. Cells are placed on untreated tissue culture plastic. Magnification of 250×.

FIG. 7. Photomicrograph of the cell monolayer on the fiber surface after a completed FEWS experiment. The cells were deposited on the tapered sensing zone of the chalcogenide fiber and exposed to 1 mM Triton for 4 h.

cells are viable for an extended period of time at the fiber surface. It can therefore be assumed that the fiber/cell system is steady over time and provides a stable basis to study the effect of toxic agent addition to the cell environment.

Figure 8b displays the membrane lipid spectral region of cells exposed to 1 mM Triton in 0.9% NaCl solution. The two main bands at 2852 cm^{-1} and 2922 cm^{-1} are attributed to CH_2 asymmetric and symmetric vibrations, respectively, and the two lower intensity bands at 2874 cm^{-1} and 2960 cm^{-1} correspond to the symmetric and asymmetric CH_3 vibrations, respectively.[19] The series of spectra in Fig. 8b correspond to different times of exposure to Triton up to a period of four hours. These spectra were baseline corrected but were not normalized. A global decrease in intensity is observed, which could be associated with the change in cell morphology shown by optical microscopy. While the cells round up, their attachment to the fiber is altered and the interaction with the evanescent wave decreases.

The second important feature that can be noted in Fig. 8b is the intensity decrease of the symmetric and asymmetric CH_2 bands relative to the CH_3 bands. In order to underline and quantify that effect, all spectra were normalized with respect to the asymmetric CH_3 band as shown in Fig. 8c. The asymmetric CH_3 vibration was arbitrarily chosen as a reference band for normalization. It should be noted that the corresponding symmetric CH_3 does not exactly mirror the behavior of the asymmetric CH_3, but rather undergoes small fluctuations. However, after normalization, a net decrease in the intensity of the CH_2 bands can be observed relative to the CH_3 bands. The decay of the CH_2 bands appears steady and continuous with time throughout the duration of the measurement.

In order to investigate the kinetics of the decay of the CH_2 bands, spectra were recorded at regular time intervals ranging from one hour before triton addition to three hours after addition. The results are presented in Fig. 9 in the form of the ratio between the CH_2 bands and the reference asymmetric CH_3 band. The band ratios were calculated by deconvoluting each spectrum into independent bands and taking the ratio of the band areas. Figure 9a shows the ratio of the symmetric CH_2 with the reference band, while Fig. 9b shows the ratio of the asymmetric CH_2 with the reference. The decay depicted in both figures is consistent and shows that the effect of Triton is mostly complete after 20 to 40 min.

Figure 9 also shows the spectral response for a range of Triton concentrations. Triton causes rapid cell damage for concentrations as low as 0.03 mM; higher concentrations do not alter the rate of cell damage significantly.

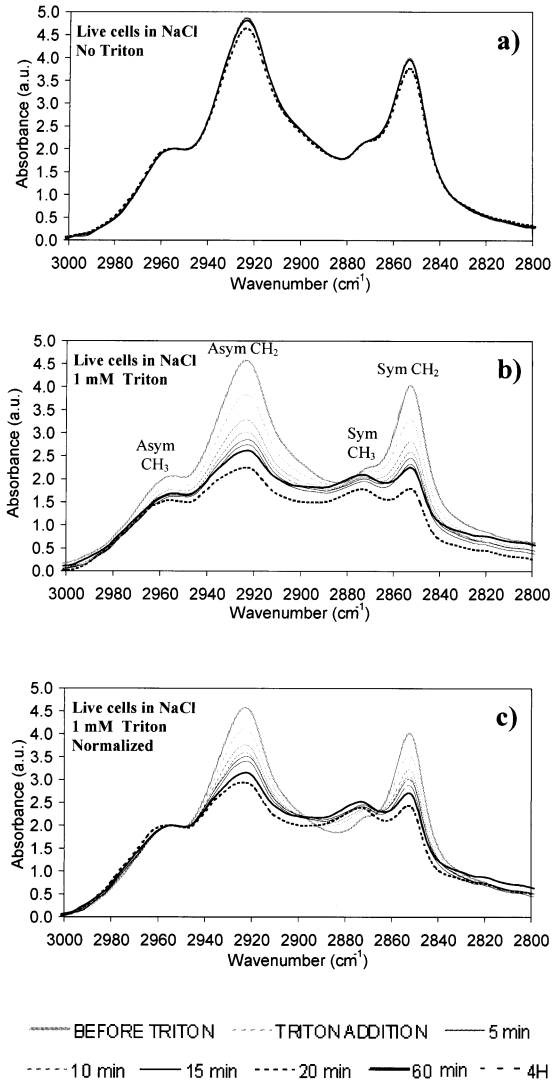

FIG. 8. FEWS spectra of human lung cells in 0.9% NaCl solution. The infrared region corresponds to the CH_2 and CH_3 vibrations of lipids. (**a**) Spectra of live cells during four hours before addition of Triton. (**b**) Spectra of live cells exposed to 1 mM Triton during four hours. (**c**) Spectra of the same experiment but spectra were normalized with respect to the asymmetric CH_3 band located around 2960 cm^{-1}.

The observed decrease in CH_2 peak intensity is systematic and reproducible for all the Triton concentrations investigated by FEWS.

The spectral response of the A549 epithelial cells was also investigated by transmission FT-IR spectroscopy. Figure 10 shows a series of transmission spectra of cells exposed to 1 mM Triton for up to 60 min. The spectral response in transmission is quite different from the FEWS experiment and only a very minor decrease in CH_2 peaks is observed. Transmission spectra were also collected for different concentrations of Triton and they all showed the same minor response. This disparity in response between the two techniques underlines the fundamental difference between transmission and evanescent wave spectroscopy.

DISCUSSION

The large variation between Figs. 8c and 10 illustrate one of the potential benefits of using FEWS versus transmission as an analytical technique for studying cell membrane integrity. The main difference between the two techniques is the spatial region of the cell that is being probed. Transmission spectroscopy probes the entire volume of the cell while FEWS offers a localized probing of the cell membrane, at least within a limited spectral region. During total internal reflection at the interface between two media of different refractive index, an electromagnetic disturbance exists in the medium beyond the reflecting interface. It is the evanescent wave whose electric field decays exponentially with distance from the interface. Using basic theoretical principles of infrared reflection spectroscopy, Harrick[6] defines the depth of penetration d_p of the evanescent wave as:

$$d_p = \frac{\lambda}{2\pi(n_2^2 \sin^2\theta_i - n_1^2)^{1/2}} \qquad (2)$$

where λ is the wavelength, n_2 and n_1 are the indices of the denser and rarer media, respectively, and θ_i is the angle of incidence of the wave in the fiber. The parameter d_p does not strictly represent the depth sampled during the IRS experiment but is rather defined as the depth at which the electric field drops to 1/e of its initial value at the surface.[20] This signifies that the major part of the signal originates from a layer of thickness d_p. Equation 2 shows that d_p is a function of the wavelength but also of the respective refractive indices and the incident angle θ_i. In a chalcogenide fiber, the limit incident angle is controlled by the numerical aperture of the fiber. Because the index of the glass is large (n_2 = 2.8) compared to the surrounding medium (n_1 = 1.3), the numerical aperture is larger than 1, and according to Snell's law, the maximum angle of propagation of a light ray coupled into a perpendicular section of the fiber is θ_t = 21°.[21] Hence, the minimum angle incident on the fiber surface is θ_i = 90 − θ_t = 69°, so that the range of possible incident

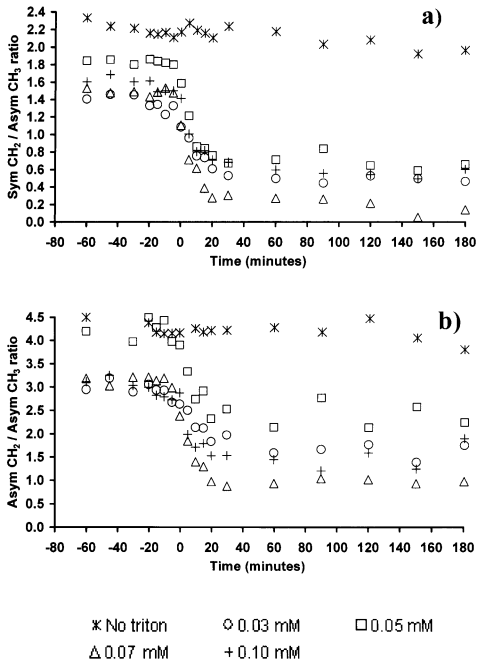

FIG. 9. Evolution of (**a**) the symmetric CH_2/asymmetric CH_3 and (**b**) asymmetric CH_2/asymmetric CH_3 ratios for various Triton concentrations (0, 0.03, 0.05, 0.07, and 0.1 mM).

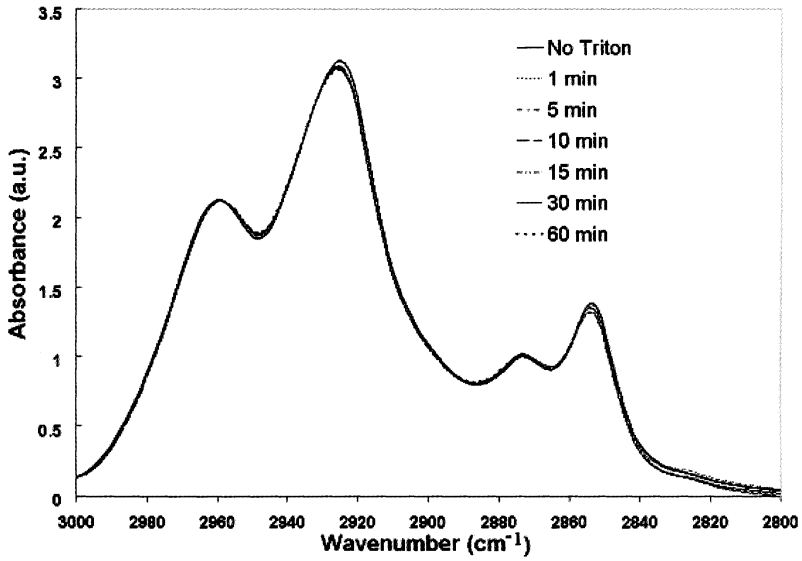

FIG. 10. Transmission FT-IR spectra of live human lung cells exposed to 1 mM Triton in a 0.9% NaCl solution.

angles is $90° \leq \theta_i < 69°$. Figure 11 shows a plot of d_p as a function of wavelength for the condition described above. The penetration depth is almost a micrometer for low wavenumbers. However, it is shown that the penetration depth becomes very small for high wavenumbers. For the spectral range of interest 2800–3000 cm^{-1}, the penetration depth reaches a maximum between 200 and 250 nm.

An important factor in the interpretation of our results lies in the strength of connection between the A549 cells and the fibers. Adherent cell types are known to have close contact to their underlying substratum only at a small number of regions. This leads to separation distances between cell surface and substrata ranging from 10 to 200 nm. The variation in separation distance is due to the presence of elongated attachment zones or focal adhesions, which are connected to the interior cytoarchitecture. The distance between cell membrane and the substrate varies from intimate contact at the focal adhesion site (<20 nm) up to several hundred nanometers. Izzard and Lochner[22] identified focal contacts with cell-to-substrate separations of 10–15 nm alongside areas of close contact with 30–50 nm separations and regions of wider separation ranging from 100–140 nm. Bereiter-Hahn et al.[23] reported focal contacts with cell-to-substrate distance of <20 nm and the most typical separation at 70 nm and between 150–200 nm. A mammalian cell membrane is typically 5–10 nm thick. The penetration depth of our IR light is on the order of 200 nm for 3000–2800 cm^{-1} light, but up to 600 nm in the signature region at 1400–1000 cm^{-1}. Therefore, our technique is probing different parts of the cell at different wavelengths, which would account for the strong membrane lipid signals found around 2900 cm^{-1} and the more complex signals from the entirety of the cell probed with longer wavelengths. Since the light penetration is on the order of 200 nm in the lipid region, we are probing mainly the 10 nm thick cell membrane and roughly 50 nm into the cytoplasm. This represents only a small portion of the cellular biomass compared with that evaluated with transmission measurements. This explains the major difference between the FEWS and the transmission signal in the lipid region because the latter

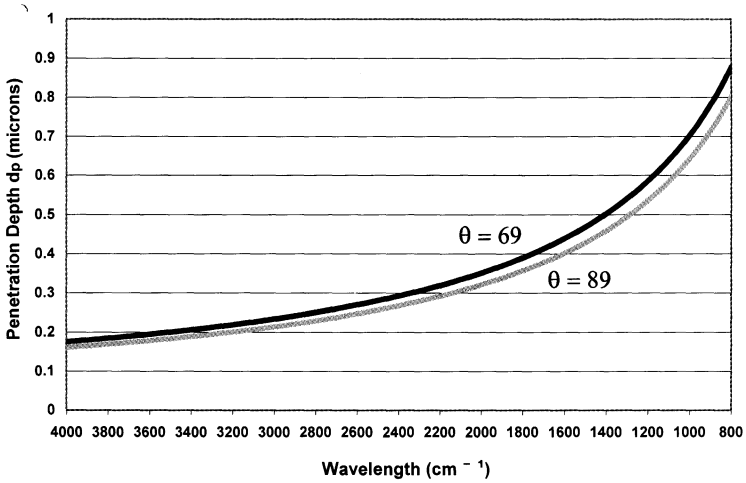

FIG. 11. Wavelength dependence of the evanescent wave penetration depth as defined by Harrick.[6] The penetration depth is shown for the range of incident angle permitted during propagation in the chalcogenide fiber.

corresponds to the sum of contribution from phospholipid membranes inside the cell including those around endosomes, endoplasmic reticulum, or golgi,[2] which are not affected by Triton. This would also explain why we do not see a significant change of the phospholipid signal in the PO_2^- stretching region at 1089 and 1242 cm^{-1},[24] because the interior of the cell is being probed in this range of wavelengths but only the plasma membrane is being damaged by Triton, and its contribution to the total lipid signal is minimal.

The Triton micelles present in the film of medium between the cell membrane and fiber surface rapidly alter the lipid bilayer as indicated by the spectral response observed in FEWS. However, the cell-to-surface attachment is not compromised and the cells adhere to the surface even through long exposure to Triton, as shown in Figs. 6 and 7. Triton is known to permeabilize the cell membrane; however, it has been demonstrated that it does not affect the focal adhesion sites of the cell.[25,26]

The results presented here demonstrate that FEWS can be employed to monitor the response of living lung cells to the presence of membrane damaging agents. Changes in the cell membrane appear more rapidly in the spectroscopic studies due to a finer time resolution available with these methods; the biochemical assays require a longer incubation time for analysis. Additionally, the spectroscopic method is more sensitive and permits the detection of membrane damage induced by Triton concentration as low as 0.03 mM. This greater sensitivity is due to the fact that FEWS directly probes the membrane vibrational modes while biochemical assays indirectly probe the effect of membrane damage such as decrease in metabolism or release of intracellular material.

This work has a number of potential extensions for the detection of biological and chemical toxins that would impact cells of the lung. For example, there is great interest in quantifying the impact of combustion-derived particulate matter (PM), such as $PM_{2.5}$ and PM_{10}, for detecting indoor inhalation health hazards, and for quantifying agents of biological warfare. The response displayed here is fairly ubiquitous in that the decay of cell membrane features does not provide information on the specific toxin that the cells have encountered. However, such a broad-range response is desirable for evaluating the presence of some unknown inhalation health hazards.

CONCLUSION

Our studies with Triton X-100, a surfactant commonly employed in biological studies, indicate that the cell membrane is altered. The cell response can be quantified through monitoring the symmetric and asymmetric CH_2 and CH_3 bands. The comparison of FEWS and transmission spectra shows that fiber spectroscopy offers an unprecedented spatial resolution to study the cell membrane. Conventional infrared microspectrometry cannot reach this resolution even with a synchrotron source.[27] The alterations observed spectroscopically are supported by traditional biochemical analyses using two cellular assays. Use of this fiber-mediated sensing of the cell response opens many possibilities for quantifying cellular response in a variety of environments outside of a laboratory setting. The measurements are very rapid and sensitive, indicating a change in cellular behavior within minutes of exposure to small concentrations of toxicant. This time and concentration resolution is significantly greater than that which could be achieved with most traditional biochemical analyses.

ACKNOWLEDGMENTS

This work was supported by DARPA contract # N66001-C-8041 and by the NIEHS sponsored Southwest Environmental Health Sciences Center # P30 ES06694.

1. D. Naumann, in *Encyclopedia of Analytical Chemistry,* R. A. Meyers, Ed. (John Wiley and Sons, Chichester, 2000), p. 102.
2. P. Lash, M. Boese, A. Pacifico, and M. Diem, Vib. Spectrosc. **28,** 147 (2002).
3. M. Diem, L. Chiriboga, P. Lasch, and A. Pacifico, Biopolymers (Biospectroscopy) **67,** 349 (2002).
4. C. P. Schultz, K. Z. Liu, J. B. Johnston, and H. H. Mantsch, J. Mol. Struct. **408/409,** 253 (1997).
5. A. Pacifico, L. A. Chiriboga, P. Lasch, and M. Diem, Vib. Spectrosc. **32,** 107 (2003).
6. N. J. Harrick, *Internal Reflection Spectroscopy* (Interscience Publishers, New York, 1967).
7. S. Hocde, C. Boussard-Pledel, G. Fonteneau, and J. Lucas, Solid State Sci. **3,** 279 (2001).
8. J. Keirsse, C. Bousard-Pledel, O. Loreal, O. Sire, B. Bureau, P. Leroyer, B. Turlin, and J. Lucas, Vib. Spectrosc. **32,** 23 (2003).
9. R. G. Crystal, J. B. West, P. J. Barnes, N. S. Cherniack, and E. R. Weible, in *The Lung: Scientific Foundations* (Raven Press, New York, 1991).
10. K. E. Driscoll, L. C. Deyo, J. M. Carter, B. W. Howard, D. G. Hassenbein, and T. A. Betram, Carcinogenesis **18,** 423 (1997).
11. B. Wallaert, O. Fahy, A. Tsicopoulos, P. Gosset, and A. B. Tonnel, Tox. Lett. **112–113,** 157 (2000).
12. C. D. Okeson, M. R. Riley, A. Fernandez, and J. O. L. Wendt, Chemosphere **51,** 1121 (2003).
13. D. Lecoq, K. Michel, G. Fonteneau, S. Hocde, C. Boussard-Pledel, and J. Lucas, Int. J. Inorg. Mat. **3,** 233 (2001).
14. S. Hocde, C. Boussard-Pledel, G. Fonteneau, D. Lecoq, H. L. Ma, and J. Lucas, J. Non-Cryst. Solids **274,** 17 (2000).
15. D. Lecoq, K. Michel, C. Boussard-Pledel, and J. Lucas, Proc. SPIE-Int. Soc. Opt. Eng. **4253,** 19 (2001).
16. R. F. Hussain, A. M. E. Nouri, and R. T. D. Oliver, J. Immunological Meth. **160,** 89 (1993).
17. M. R. Riley, D. E. Boesewetter, A. M. Kim, and F. P. Sirvent, Toxicology **190,** 171 (2003).
18. A. K. Chibisov, T. D. Slavnova, and H. Gorner, J. Photochem. Photobiol., B **72,** 11 (2003).
19. B. Rigas, S. Morgello, I. S. Goldman, and P. T. T. Wong, Proc. Natl. Acad. Sci. U.S.A. **87,** 8140 (1990).
20. F. M. Mirabella, Appl. Spectrosc. Rev. **21,** 45 (1985).
21. E. Hecht, *Optics* (Addison-Wesley, Reading, MA, 1987).
22. C. S. Izzard and L. R. Lochner, J. Cell Sci. **21,** 139 (1976).
23. J. Bereither-Hahn, C. H. Fox, and B. Thorell, J. Cell Biology **82,** 767 (1979).
24. A. Pevsner and M. Diem, Biopolymer (Biospectroscopy) **72,** 282 (2003).
25. R. G. Richards, M. Stiffanic, G. R. H. Owen, M. Riehle, I. A. P. Gwynn, and A. S. G. Curtis, Cell Biol. Int. **25,** 1237 (2001).
26. M. Niederreiter, M. Gimona, F. Streichsbier, J. E. Celis, and J. V. Small, Electrophoresis **15,** 511 (1994).
27. N. Jamin, P. Dumas, J. Moncuit, W. H. Fridman, J. L. Teillaud, G. Lawrence Carr, and G. P. Williams, Proc. Natl. Acad. Sci. U.S.A. **95,** 4837 (1998).